Human Vam6p promotes lysosome clustering and fusion in vivo

Steve Caplan,[1] Lisa M. Hartnell,[1] Rubén C. Aguilar,[1] Naava Naslavsky,[2] and Juan S. Bonifacino[1]

[1]Cell Biology and Metabolism Branch at the National Institute of Child Health and Human Development and [2]Laboratory of Cell Biology at the National Heart, Lung and Blood Institute, National Institutes of Health, Bethesda, MD 20892

Regulated fusion of mammalian lysosomes is critical to their ability to acquire both internalized and biosynthetic materials. Here, we report the identification of a novel human protein, hVam6p, that promotes lysosome clustering and fusion in vivo. Although hVam6p exhibits homology to the *Saccharomyces cerevisiae* vacuolar protein sorting gene product Vam6p/Vps39p, the presence of a citron homology (CNH) domain at the NH$_2$ terminus is unique to the human protein. Overexpression of hVam6p results in massive clustering and fusion of lysosomes and late endosomes into large (2–3 μm) juxtanuclear structures. This effect is reminiscent of that caused by expression of a constitutively activated Rab7. However, hVam6p exerts its effect even in the presence of a dominant-negative Rab7, suggesting that it functions either downstream of, or in parallel to, Rab7. Data from gradient fractionation, two-hybrid, and coimmunoprecipitation analyses suggest that hVam6p is a homooligomer, and that its self-assembly is mediated by a clathrin heavy chain repeat domain in the middle of the protein. Both the CNH and clathrin heavy chain repeat domains are required for induction of lysosome clustering and fusion. This study implicates hVam6p as a mammalian tethering/docking factor characterized with intrinsic ability to promote lysosome fusion in vivo.

Introduction

Membrane-bound organelles of the endocytic and secretory pathways are continuously undergoing regulated fusion and fission events that allow exchange of materials between them. Before fusion, the organelles are brought in close proximity by various tethering and docking factors (for review see Waters and Pfeffer, 1999). This proximity enables the action of a fusion machinery composed of NSF, SNAPs, SNAREs, and other associated proteins (Sollner and Rothman, 1996). Members of the Rab family of small GTP-binding proteins play roles in the recruitment of tethering/docking factors and/or their coupling to the fusion machinery (Novick and Zerial, 1997). The specificity of fusion arises from the particular combination of tethering/docking factors, SNAREs, and Rabs that can be assembled at sites of fusion. Tethering/docking factors involved in different transport steps tend to be step specific and often bear little structural resemblance to one another. SNAREs and Rabs involved in those steps, on the other hand, are structurally

related (Waters and Pfeffer, 1999). This suggests that once specific tethering/docking has occurred, fusion ensues by a conserved mechanism.

Fusion of mammalian lysosomes with other membrane-bound organelles is key to their ability to acquire both internalized and biosynthetic materials (Kornfeld and Mellman, 1989; Luzio et al., 2000). Lysosomes have been shown to fuse with late endosomes (Mullock et al., 1998; Pryor et al., 2000; Ward et al., 2000) and phagosomes (Zimmerli et al., 1996; Funato et al., 1997) (heterotypic fusion), as well as with themselves (Bakker et al., 1997; Ward et al., 1997, 2000) (homotypic fusion). Late endosome–lysosome fusion, in particular, has been the subject of much interest in recent years. Late endosomes have been proposed to establish transient contacts with lysosomes (i.e., kiss-and-run; Storrie and Desjardins, 1996) or to undergo complete fusion into a hybrid organelle from which lysosomes are later recovered by a fission event (i.e., fusion–fission; Mullock et al., 1998; Pryor et al., 2000). Although the occurrence of lysosome fusion has been extensively documented, the identification of factors involved in this process, particularly in the specific tethering and/or docking events, is still in its infancy. In vitro studies of late endosome–lysosome fusion have revealed a requirement for ATP, NSF, SNAPs, Rabs, as well as the SNARE syntaxin 7 (Mullock et al., 1998, 2000; Pryor et al., 2000; Ward et al., 2000), whereas in vivo overexpression

studies have suggested a role for Rab7 (Bucci et al., 2000). To date, no tethering/docking factors have been identified that play a role in mammalian lysosome fusion.

Potential candidates for lysosomal tethering/docking factors are mammalian homologues of *Saccharomyces cerevisiae* gene products involved in vacuole fusion (for review see Wickner and Haas, 2000). Among these are Vps11p, Vps18p, Vps16p, Vps33p, Vam2p/Vps41p, and Vam6p/Vps39p, which assemble on the vacuolar membrane into a complex referred to as homotypic fusion and vacuole protein sorting (HOPS)* (Eitzen et al., 2000; Seals et al., 2000; Ungermann et al., 2000) or C-Vps complex (Sato et al., 2000; Wurmser et al., 2000). This complex has been shown to cooperate with the yeast homologue of mammalian Rab7, Ypt7p, to enable vacuole fusion mediated by the SNAREs (Ungermann et al., 1999, 2000; Eitzen et al., 2000; Sato et al., 2000; Seals et al., 2000; Wurmser et al., 2000). In this study, we report the identification and characterization of a human homologue of *S. cerevisiae* Vam6p/Vps39p (Nakamura et al., 1997), which we refer to as hVam6p. We show that overexpression of this protein in human cells induces massive clustering and fusion of lysosomes, whereas early endosomes and other organelles of the endocytic and secretory pathways remain unaffected. hVam6p exerts these effects by associating with the cytoplasmic face of the lysosomal membrane. An NH_2-terminal citron homology (CNH) domain and a central clathrin homology (CLH) repeat domain in hVam6p are required for lysosome clustering and fusion. These observations suggest that hVam6p may function as a tethering/docking factor specifically involved in lysosome fusion.

Results

Identification and domain organization of human Vam6

A novel human cDNA encoding a protein homologous to the *S. cerevisiae* vacuolar protein sorting gene product Vam6p/Vps39p (Nakamura et al., 1997) was identified through searches of DNA databases and 5′ RACE-PCR (Fig. 1 A). This cDNA encodes a protein designated hVam6p of 886 amino acid residues and a predicted molecular mass of ~100 kD. hVam6p bears 26% identity and 42% overall amino acid sequence homology to the COOH-terminal region of *S. cerevisiae* Vam6p (Fig. 1, A and B). Homologues of hVam6p were also identified in *Drosophila melanogaster* (35% identity, 53% homology), *Caenorhabditis elegans* (30% identity, 50% homology) (Fig. 1, A and B), and *Schizosaccharomyces pombe* (24% identity, 41% homology) (Fig. 1 B). Our searches also identified a second human homologue of *S. cerevisiae* Vam6p that had already been characterized as the TGF-β receptor-I–associated protein-1 (TRAP-1) (21% identity, 40% homology) (Charng et al., 1998) (Fig. 1 B).

Theoretical analyses predict the presence of a CNH domain (Madaule et al., 1995) near the NH_2 terminus of hVam6p, TRAP-1, and their *S. pombe*, *D. melanogaster*, and

C. elegans homologues (Fig. 1, A and B). Although these proteins exhibit significant homology to hVam6p throughout the entire protein (Fig. 1 B, gray shaded blocks), the *S. cerevisiae* Vam6p lacks a defined CNH domain, and the region of significant homology commences only after the first 450 residues. CNH domains also exist near the COOH terminus of several kinases involved in the jun kinase (JNK) activation pathway (e.g., NIK and TNIK) and of the *S. cerevisiae* Rho guanine nucleotide exchange factor Rom1p (Fig. 1 B). Little is known about the function of this domain, although it has been proposed to regulate kinase activity (Fu et al., 1999; Dan et al., 2000) and to mediate binding to the GTP-bound forms of Rac and Rho (Madaule et al., 1995).

hVam6p and its homologues also contain a CLH motif (Fig. 1, A and B) similar to seven such motifs present in the leg domain of the clathrin heavy chain (Ybe et al., 1999). Similar motifs are also found in the *S. cerevisiae* vacuolar sorting proteins Vam2p/Vps41p (Fig. 1 B), Vps18p, Vps11, and Vps8p. These motifs have been proposed to mediate protein–protein interactions leading to homo- or heterooligomerization of the proteins (Ybe et al., 1999; Darsow et al., 2001).

Northern blot analysis demonstrated that hVam6p mRNA is expressed in all human tissues examined (Fig. 1 C), indicating that the protein may be widely expressed.

Coalescence of lysosomes and late endosomes caused by overexpression of hVam6p

S. cerevisiae Vam6p has been implicated in tethering and/or docking events that precede homotypic vacuole fusion (Eitzen et al., 2000; Price et al., 2000a,b; Seals et al., 2000; Wurmser et al., 2000). To assess whether hVam6p could play a similar role in lysosome tethering/docking, we examined the effects of overexpressing Myc epitope–tagged hVam6p (Myc–hVam6p) by transient transfection into HeLa cells. Fixed-permeabilized cells were analyzed by indirect immunofluorescence microscopy after double labeling with antibodies to the Myc epitope and to the lysosomal integral membrane proteins, lamp-1 (Fig. 2, A–C), lamp-2 (Fig. 2, D–F), and CD63 (Fig. 2, G–I). Untransfected cells exhibited the characteristic distribution of lysosomes, which were more concentrated in the juxtanuclear area of the cytoplasm but also extended toward the cell periphery (Fig. 2, A–I). In contrast, cells overexpressing hVam6p displayed a striking coalescence of lysosomes into a few large juxtanuclear structures (Fig. 2, A–I, arrows) with concomitant loss of peripheral lysosomes. These large structures were observed in virtually all hVam6p-overexpressing cells and contained all three lysosomal membrane proteins tested, as well as the lysosomal luminal hydrolase, cathepsin D (Fig. 2, J–L, arrows). The distributions of the early endosomal marker, transferrin receptor, in cells overexpressing hVam6p (Fig. 2, M–O, arrowhead), as well as various other endosomal, TGN, and Golgi markers (i.e., EEA1, AP-1, and the 58-kD Golgi protein; data not shown), were not affected. These observations suggested that the morphological alterations induced by overexpression of hVam6p were specific to organelles containing lysosomal membrane and luminal proteins.

The exogenously expressed hVam6p appeared to be mostly cytosolic (Fig. 2, B, E, H, K, and N). To determine whether the cytosolic pool could have masked a population

---

*Abbreviations used in this paper: CI-MPR, cation-independent mannose-6-phosphate receptor; CLH, clathrin homology; CNH, citron homology; GAL4ad, GAL4 transcription activation domain; GAL4bd, GAL4 DNA–binding domain; GFP, green fluorescent protein; HOPS, homotypic fusion and vacuole protein sorting; TRAP-1, TGF-β receptor-I–associated protein-1.
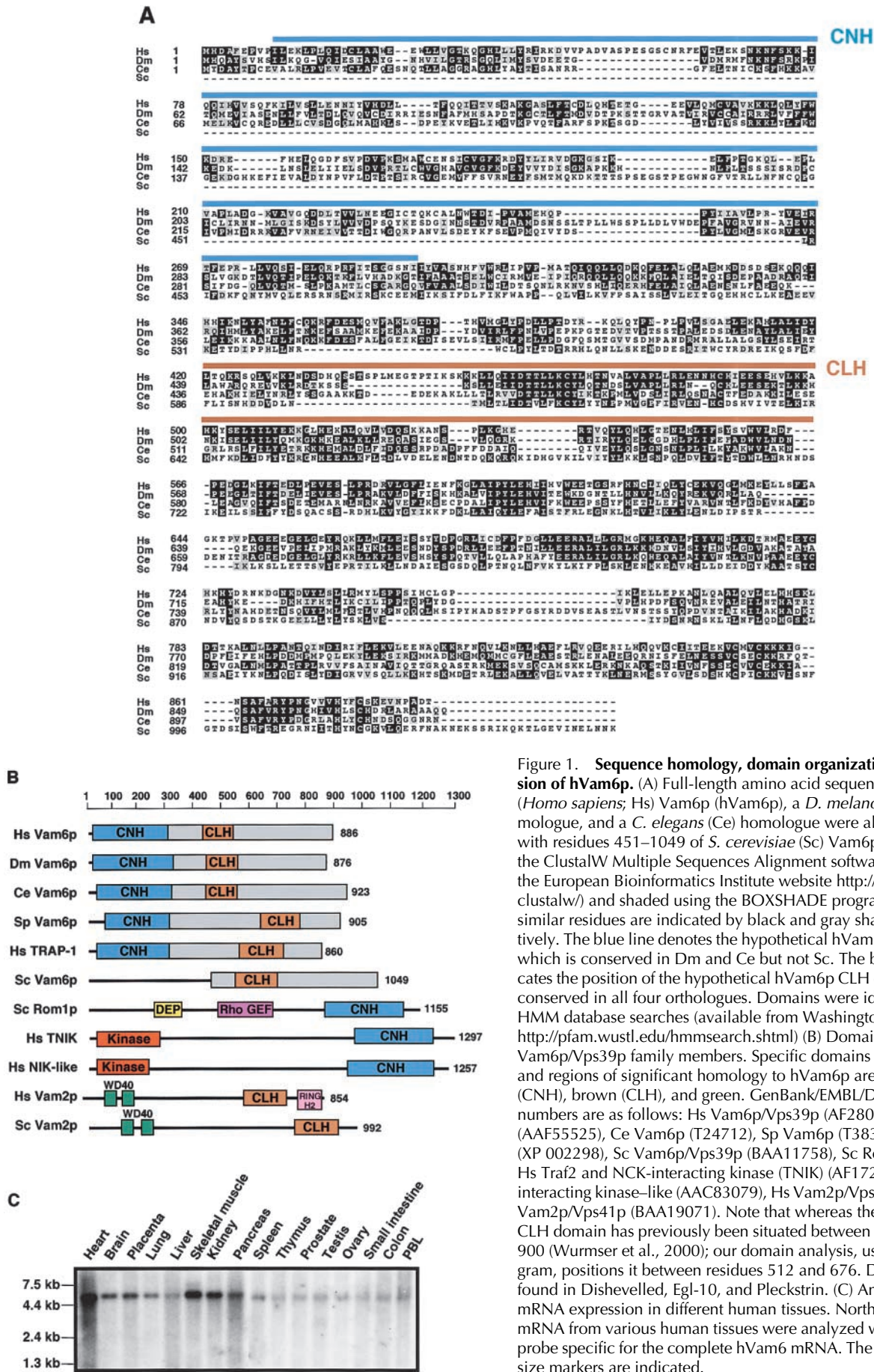
Figure 1. **Sequence homology, domain organization, and expression of hVam6p.** (A) Full-length amino acid sequences of human (*Homo sapiens*; Hs) Vam6p (hVam6p), a *D. melanogaster* (Dm) homologue, and a *C. elegans* (Ce) homologue were aligned together with residues 451–1049 of *S. cerevisiae* (Sc) Vam6p/Vps39p, using the ClustalW Multiple Sequences Alignment software (available at the European Bioinformatics Institute website http://www2.ebi.ac.uk/clustalw/) and shaded using the BOXSHADE program. Identical and similar residues are indicated by black and gray shading, respectively. The blue line denotes the hypothetical hVam6p CNH domain, which is conserved in Dm and Ce but not Sc. The brown line indicates the position of the hypothetical hVam6p CLH domain, which is conserved in all four orthologues. Domains were identified by Pfam HMM database searches (available from Washington University at http://pfam.wustl.edu/hmmsearch.shtml) (B) Domain organization of Vam6p/Vps39p family members. Specific domains are color-coded and regions of significant homology to hVam6p are shown in blue (CNH), brown (CLH), and green. GenBank/EMBL/DDBJ accession numbers are as follows: Hs Vam6p/Vps39p (AF280814), Ds Vam6p (AAF55525), Ce Vam6p (T24712), Sp Vam6p (T38314), Hs TRAP-1 (XP 002298), Sc Vam6p/Vps39p (BAA11758), Sc Rom1p (S64365), Hs Traf2 and NCK-interacting kinase (TNIK) (AF172270), Hs NCK-interacting kinase–like (AAC83079), Hs Vam2p/Vps41p (P49754), Sc Vam2p/Vps41p (BAA19071). Note that whereas the *S. cerevisiae* CLH domain has previously been situated between residues 716 and 900 (Wurmser et al., 2000); our domain analysis, using the Pfam program, positions it between residues 512 and 676. DEP is a domain found in Dishevelled, Egl-10, and Pleckstrin. (C) Analysis of hVam6 mRNA expression in different human tissues. Northern blots with mRNA from various human tissues were analyzed with a ^{32}P-labeled probe specific for the complete hVam6 mRNA. The positions of RNA size markers are indicated.
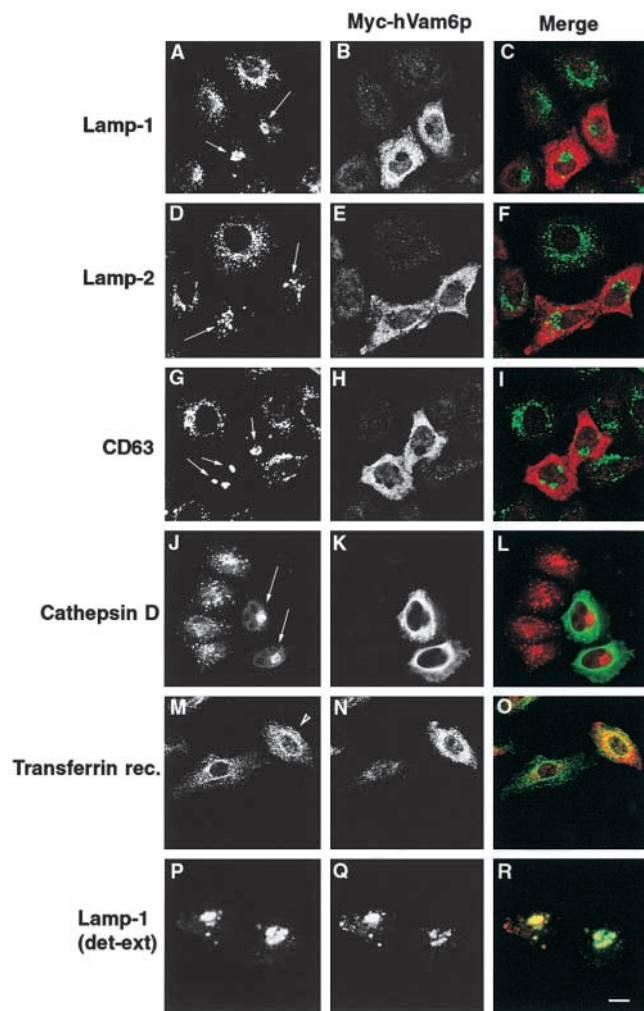
Figure 2. **Overexpression of hVam6p induces coalescence of lysosomal vesicles.** (A–O) HeLa cells were transiently transfected with a plasmid encoding Myc–hVam6p. Cells were fixed, permeabilized, and incubated with rabbit polyclonal antibodies to the Myc epitope together with mouse monoclonal antibodies to lamp-1 (A–C), lamp-2 (D–F), CD63 (G–I), or transferrin receptor (M–O), or rabbit polyclonal antibody to cathepsin D (J–L). Arrows (A, D, G, and J) indicate the coalescence of lysosomes into large juxtanuclear structures. Arrowhead (M) indicates a transfected cell. (P–R) HA–hVam6p-transfected HeLa cells were extracted for 1 min with 0.05% (wt/vol) saponin before fixation. Cells were then fixed and incubated with rabbit polyclonal antibodies to the HA epitope, together with mouse monoclonal antibodies to lamp-1. Bound antibodies were revealed by Cy3-conjugated donkey anti–rabbit IgG (red channel) and Alexa-488–conjugated donkey anti–mouse antibody (green channel). Bar, 10 μm.

of membrane-associated hVam6p, we performed immunofluorescence microscopy of hVam6p-expressing HeLa cells after extraction of the cytosol with 0.05% wt/vol saponin before fixation. This procedure uncovered the presence of hVam6p on the same large lysosomal structures that contained lamp-1 (Fig. 2, P–R).

The localization of hVam6p in transfected HeLa cells was further examined by immunoelectron microscopy of ultrathin frozen sections (Fig. 3). hVam6p was found to be associated with an electron dense halo surrounding 0.2–0.6 μm vesicles that were part of large clusters (Fig. 3 A, 10-nm gold particles, arrows). All of these vesicles were also labeled

for the lysosomal membrane protein, lamp-2 (Fig. 3 A, 15-nm gold particles, arrowheads). Although many hVam6p-coated vesicles did not contain cation-independent mannose 6-phosphate receptor (CI-MPR) (Fig 3 B, *), others contained both hVam6p (Fig. 3 B, 10-nm gold particles, arrows) and CI-MPR (Fig. 3 B, 15-nm gold particles, arrowhead), and some had the appearance of multivesicular bodies. Together, these observations suggest that hVam6p associates with and induces clustering of lysosomes and late endosomes.

Functional assessment of hVam6p-induced lysosomal structures

The hVam6p-induced lysosomal structures could be labeled with the acidotropic fluorescent probe, LysoTracker red, indicating that they were acidic (Fig. 4, A–C, arrow). To determine if they were also accessible to fluid-phase markers, HeLa cells expressing Myc–hVam6p were allowed to internalize the fluid phase marker rhodamine–dextran for various time periods. Cells were then fixed permeabilized cells and subjected to indirect immunofluorescence to detect hVam6p-expressing cells. At time points ranging from 15 min (not shown) to 1 h (Fig. 4, D–F), rhodamine–dextran was found to be internalized equally well into typical lysosomes in untransfected cells and lysosomal clusters in hVam6p-transfected cells (Fig. 4 D, arrows), suggesting no major change in accessibility to fluid phase markers upon expression of hVam6p.

To determine whether hVam6p-induced structures were also capable of degrading protein cargo, we cotransfected cells with a Tac fusion protein containing a dileucine-based endocytic and lysosomal targeting signal, Tac-DKQTLL, (Letourneur and Klausner, 1992), together with either hVam6p or nonmyristylated Arf6 as a control. Pulse–chase analysis of Tac-DKQTLL subsequent to both metabolic and cell surface labeling demonstrated that cells transfected with hVam6p were capable of degrading proteins with kinetics similar to normal cells (Fig. 4 G). All of these observations suggested that hVam6p-induced lysosomal structures, despite their altered morphology, were still capable of receiving and degrading materials delivered from the endocytic system.

Ultrastructural analysis of hVam6p-induced lysosomal structures loaded with internalized HRP

We took advantage of the ability to load the hVam6p-induced lysosomal structures with fluid phase endocytic markers to analyze their ultrastructure in more detail. Untransfected or hVam6p-transfected HeLa cells were allowed to internalize HRP for 4 h. After standard fixation, diaminobenzidine development for HRP visualization, and resin embedding, cell sections were analyzed by electron microscopy. As expected, untransfected cells displayed an array of 0.2–0.6-μm HRP-positive vesicles scattered throughout the cytoplasm, most of which likely corresponded to late endosomes and lysosomes because of the long period of internalization (Fig. 5 A). hVam6p-transfected HeLa cells, on the other hand, contained at least three types of abnormal structures. The first type consisted of large clusters of HRP-positive 0.2–0.6 μM vesicles, most of which contained intraluminal vesicles or other membranous inclusions (Fig. 5, B and C), similar to those seen on
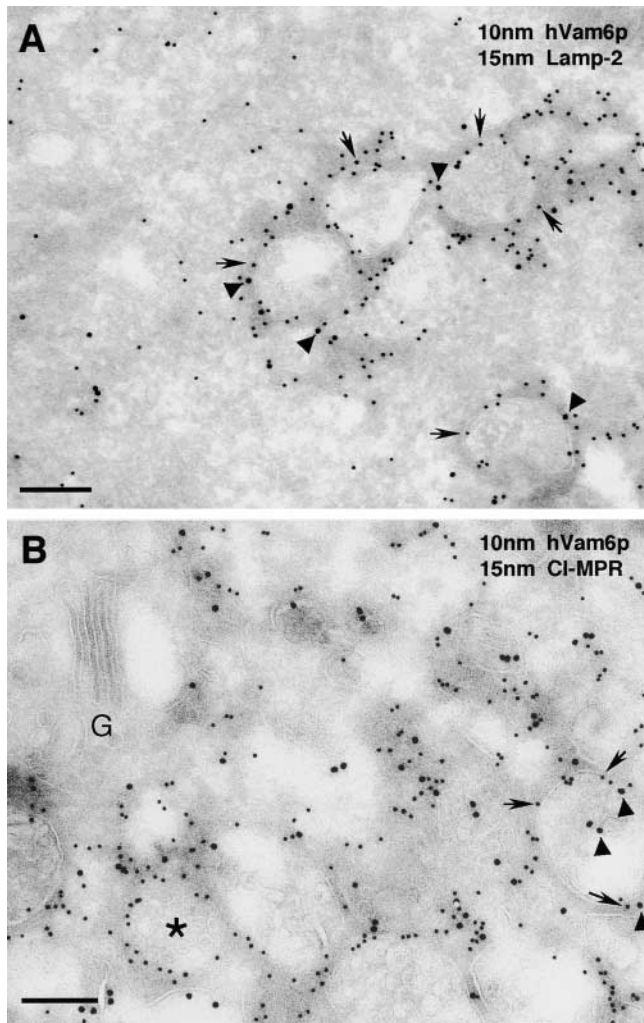
Figure 3. Association of hVam6p with clusters of lysosomes and late endosomes. HeLa cells were transiently transfected with HA–hVam6p and processed for immunoelectron microscopy. Ultra-thin frozen sections were labeled with antibodies to HA (to detect hVam6p) and either endogenous lamp-2 (A) or endogenous CI-MPR (B). Bound antibodies were detected using conjugated protein A–gold. Arrows indicate the localization of hVam6p to a halo around the membranes of lysosomes and late endosomes (A and B, 10-nm gold particles), whereas arrowheads indicate the localization of lamp-2 (A, 15-nm gold particles) or CI-MPR (B, 15-nm gold particles), and the asterisk marks a structure labeled only for hVam6p. G, Golgi. Bars, 0.2 μm.

ultrathin cryosections (Fig. 3). The second type of abnormal structures were large (2–3 μm) vacuoles (Fig. 5, B and D). Some of these vacuoles seemed empty, displaying the appearance of swollen vacuoles. Others had variable amounts of HRP-positive materials, including 0.2–0.6 μM vesicles, within their interior (Fig. 5 D). The third type was a combination of the former two in that clusters of 0.2–0.6-μM HRP-positive vesicles were docked onto the membranes of the large vacuoles (Fig. 5, B and E). Serial sectioning (not shown) revealed that these three types of structures were situated next to the nucleus, often nestled between nuclear lobes. These analyses suggested a possible series of events induced by hVam6p, in which late endosomes and lysosomes first cluster together and then undergo fusion to generate large vacuoles.

Dynamics of lysosome clustering and fusion induced by hVam6p

To investigate the processes that led to the formation of lysosomal clusters and large vacuoles over time, we monitored the movement of lysosomes in live cells by time-lapse fluorescence microscopy. To this aim, COS-7 and HeLa cells were transfected with plasmids encoding green fluorescent protein (GFP)–lamp-1 alone or GFP–lamp-1 and hVam6p. In cells transfected with GFP–lamp-1 alone, lysosomes and/or late endosomes exhibited bidirectional movement between the juxtanuclear area and sites in the cell periphery (data not shown). In the doubly transfected cells, the effects of hVam6p on lysosomes were concurrent with the expression of GFP–lamp-1, which made it necessary to image cells already displaying incipient lysosome clustering. At early time points, we could observe peripheral lysosomes moving centripetally toward the center of the cell and attaching to or merging with other lysosomes (Fig. 6 A, arrow, Video 1). More centrally located lysosomes were also observed to cluster and/or fuse with one another (Fig. 6 A, arrowhead, and B; Videos 1 and 2). Over time, these clustering and fusion events lead to the accumulation of large lysosomal structures in the juxtanuclear area (Fig. 6 C; Video 3). These observations suggested that hVam6p causes lysosomes and late endosomes to stick together in tight clusters and fuse, thus preventing them from migrating back to the cell periphery. (Videos 1, 2, and 3 are available at http://www.jcb.org/cgi/content/full/200102142/DC1.)

Treatment of HeLa cells with 0.5 μM nocodazole immediately after transfection with an hVam6p-encoding plasmid did not impede the coalescence of lamp-1–containing structures in the cell periphery but did prevent their translocation to the juxtanuclear area of the cell (Fig. 6 D). This indicated that microtubules are not involved in the clustering process itself but in the localization of the clusters to the juxtanuclear area.

Functional relationship of hVam6p to Rab7

The effects of hVam6p on lysosomes are reminiscent of those elicited by a constitutively active Rab7 Q67L mutant (Bucci et al., 2000). To determine whether Rab7 nucleotide cycling is necessary for the formation of hVam6p-induced lysosome clusters, we transfected cells with wild-type GFP–Rab7, constitutively activated GFP–Rab7 Q67L, or dominant-negative GFP–Rab7 T22N, each alone or together with hVam6p. Overexpression of wild type GFP–Rab7 did not affect the distribution of endogenous lamp-1 (Fig. 7, A and B) as previously reported (Bucci et al., 2000). However, in cells transfected with GFP–Rab7 and hVam6p, both GFP–Rab7 and lamp-1 were found in large juxtanuclear clusters (Fig. 7, C and D, arrowheads). Since GFP–Rab7 Q67L induces an effect on lysosomes (Bucci et al., 2000) that resembles that of hVam6p, we were unable to discern any additional effect in cells expressing both of these proteins (data not shown). However, GFP–Rab7 T22N, which by itself causes dispersal of lysosomes from the juxtanuclear region to the periphery (Bucci et al., 2000; and Fig. 7, E and F, small arrows) did not block the coalescence of lysosomes induced by hVam6p (Fig. 7, G and H, large arrow). These findings imply that hVam6p exerts its affects either downstream of or in parallel to Rab7.

hVam6p   Merge

Figure 4. Functional characterization of hVam6p-induced lysosomal clusters. (A–F) Live HeLa cells transiently transfected with Myc–hVam6p were incubated with LysoTracker red (A–C) or rhodamine–dextran (D–F) for 1 h, and then fixed-permeabilized. Cells were incubated with a mouse monoclonal antibody to Myc, followed by Alexa-488–conjugated donkey antibody to mouse IgG (B and E, green channel). The LysoTracker red and rhodamine–dextran are visible in the red channel (A and D). Arrows denote the accumulation of acidotropic (A) and fluid phase (D) markers within clustered lysosomes in hVam6p-transfected cells. Bar, 10 μm. (G) HeLa cells were cotransfected with either Tac-DKQTLL and Myc–hVam6p, or Tac-DKQTLL and a nonmyristylated Arf6 control. After 24 h, cotransfection efficiency was monitored by indirect immunofluorescence (as described in the legend to Fig. 2), and cells were pulsed for 30 min either by metabolic labeling (top) or cell surface biotinylation (bottom). The cells were then chased for the time points indicated, harvested, lysed, subjected to immunoprecipitation analysis using antibodies directed against Tac, and resolved on 4–20% SDS-PAGE. Samples from metabolically labeled and biotinylated cells were visualized by autoradiography and blotting with streptavidin–HRP, respectively.
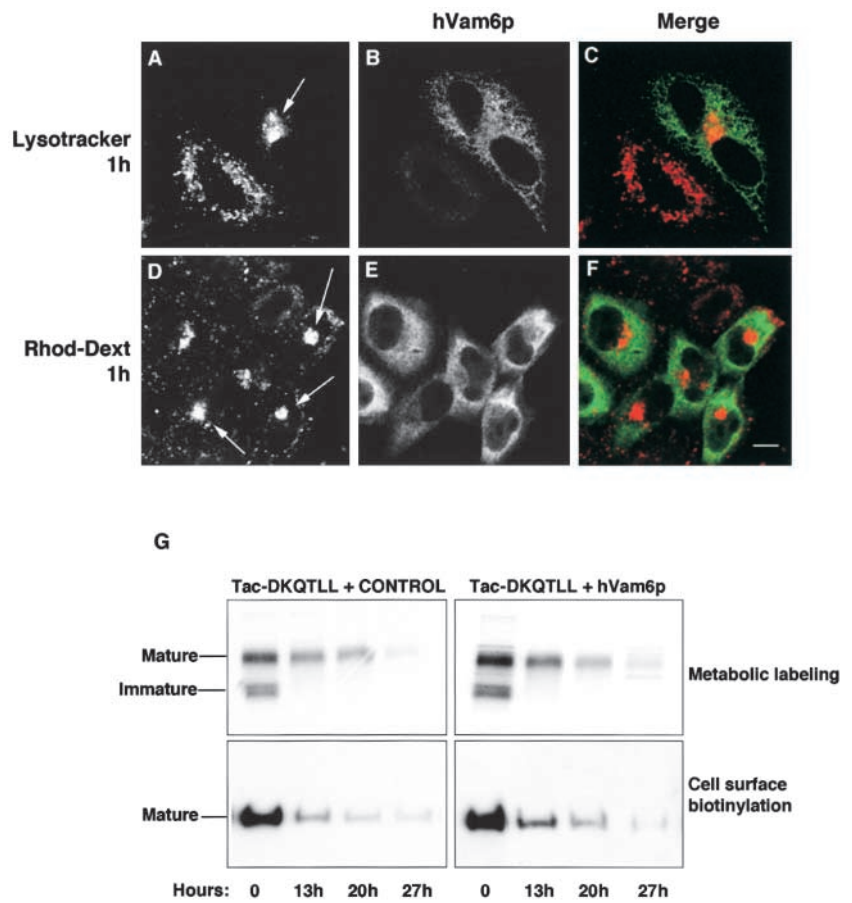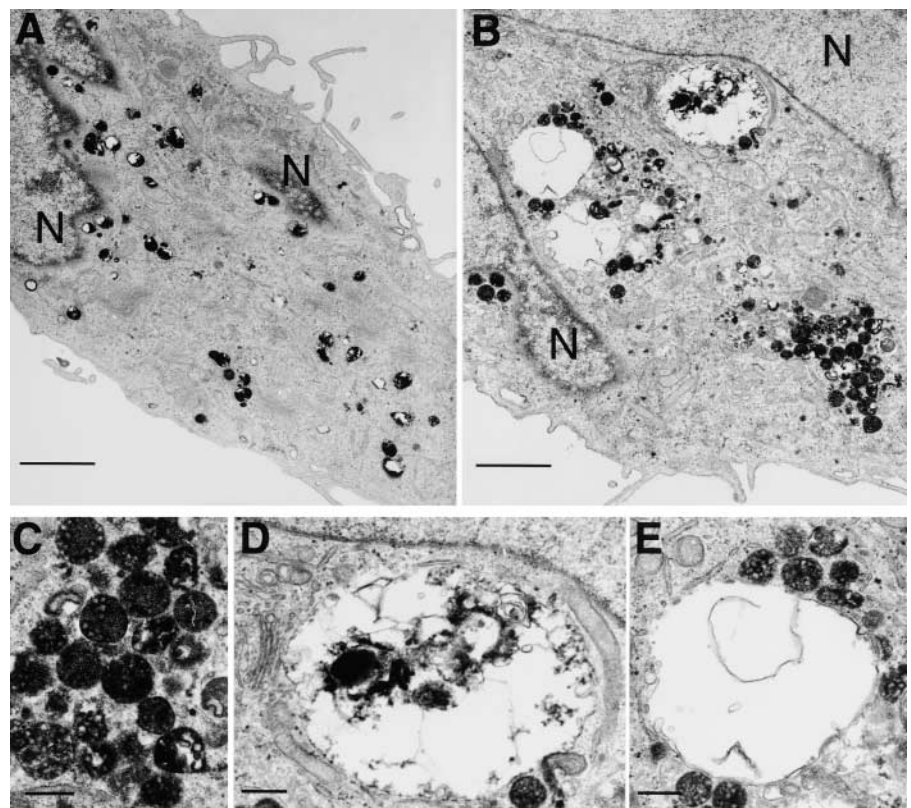
Figure 5. Ultrastructural analysis of hVam6p-induced lysosomal structures labeled with internalized HRP. Untransfected (A) or hVam6p-transfected (B–E) HeLa cells were subjected to a continuous 4 h fluid phase uptake of HRP 24 h after transfection. (A) In control cells, HRP-containing lysosomes and endosomes were small (0.2–0.6 μm) and distributed throughout cell. (B) In hVam6p-transfected cells, clusters of multivesicular HRP-positive vesicles (enlarged in C) and large (2–3 μm) vacuoles situated next to the nucleus were visible. Some of these large vacuoles contained HRP (enlarged in D), whereas others appeared to have smaller HRP-positive vesicles docking onto their membrane (enlarged in E). N, Nucleus. Bars: (A and B) 2 μm; (C–E) 0.4 μm.
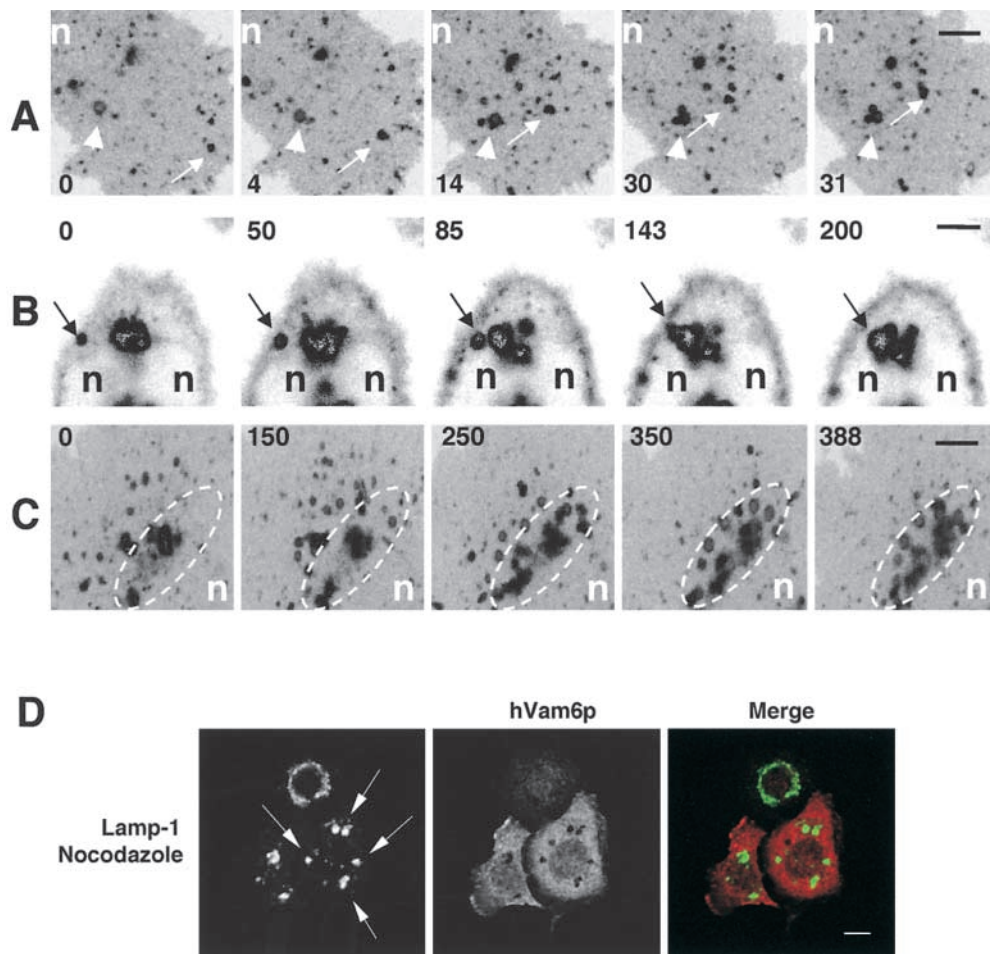
Figure 6. **Dynamics of hVam6p-induced lysosome clustering and fusion.** COS-7 (A and C) or HeLa (B) cells were transfected with plasmids encoding GFP–lamp-1 (GFP–lgp120) and HA–hVam6p. 10 h after transfection, live cells were incubated at 37°C and scanned for GFP-expressing cells by confocal microscopy. Live images were acquired at 30-s time intervals and are displayed as inverted images with the time in minutes relative to the start of imaging indicated in the lower left corner (A) or upper left corner (B and C). The dotted oval region of interest (C) outlines juxtanuclear regions that accumulate lysosome clusters and giant lysosomes. Arrows (A and B) point at moving vesicles. Arrowheads (A) point at a lysosome clustering event. n, nucleus. (D) Microtubule depolymerization impairs formation of a unified, giant juxtanuclear lysosomal structure in hVam6p-transfected cells. HeLa cells were transfected with Myc-hVam6p and treated with 0.5 μM nocodazole for 16 h. Cells were then fixed-permeabilized, incubated with a rabbit polyclonal antibody to Myc and a mouse monoclonal antibody to lamp-1, followed by Alexa-488–conjugated donkey antibody to mouse IgG (left, green channel) and Cy3-conjugated donkey anti–rabbit IgG (middle, red channel). Bars, (A and C) 5 μm; (B) 10 μm. Quicktime movie sequence versions of this figure are available at http://www.jcb.org/cgi/content/full/200102142/DC1.

Homooligomerization of hVam6p

A novel Rab7 effector termed RILP (Cantalupo et al., 2001) has recently been identified through its binding to the constitutively active Rab7 Q67L and has been demonstrated to mediate the effects of Rab7 on lysosome biogenesis. To determine whether hVam6p interacts with either Rab7 Q67L or RILP, we used a yeast two-hybrid approach. As expected, Rab7 Q67L and RILP interacted with one another (Cantalupo et al., 2001; and Fig. 8 A). However, neither Rab7 Q67L nor RILP displayed an interaction with hVam6p, consistent with the idea that hVam6p acts independently of Rab7. A strong interaction was observed upon coexpression of GAL4 transcription activation domain (GAL4ad)–hVam6p and GAL4 DNA–binding domain (GAL4bd)–hVam6p (Fig. 8 A), however, suggesting that hVam6p may be able to self-assemble.

To determine the size of potential hVam6p oligomers in vivo, HA–hVam6p-transfected HeLa cells were labeled for

8 h with [^{35}S]methionine, extracted with detergent, fractionated by ultracentrifugation on a 5–20% sucrose gradient, and analyzed by immunoprecipitation with anti-HA antibodies (Fig. 8 B). A major species of ∼105 kD was detected on SDS-PAGE of anti-HA immunoprecipitates, in good agreement with the predicted molecular mass of hVam6p (∼100 kD). HA–hVam6p peaked in gradient fractions corresponding to a molecular mass of ∼317 kD, higher than the molecular mass of the adaptor protein complex AP-2 (∼270 kD). This indicated that hVam6p is a component of an oligomeric complex. Since no other major bands were detected in the immunoprecipitates (Fig. 8 B), these results suggest that hVam6p is a homooligomer, most likely a homotrimer.

To further assess the self-association of hVam6p in vivo, HeLa cells were cotransfected with Myc–hVam6p and HA–hVam6p (Fig. 9 B). After metabolic labeling, the cells were lysed and subjected to immunoprecipitation–recapture anal-
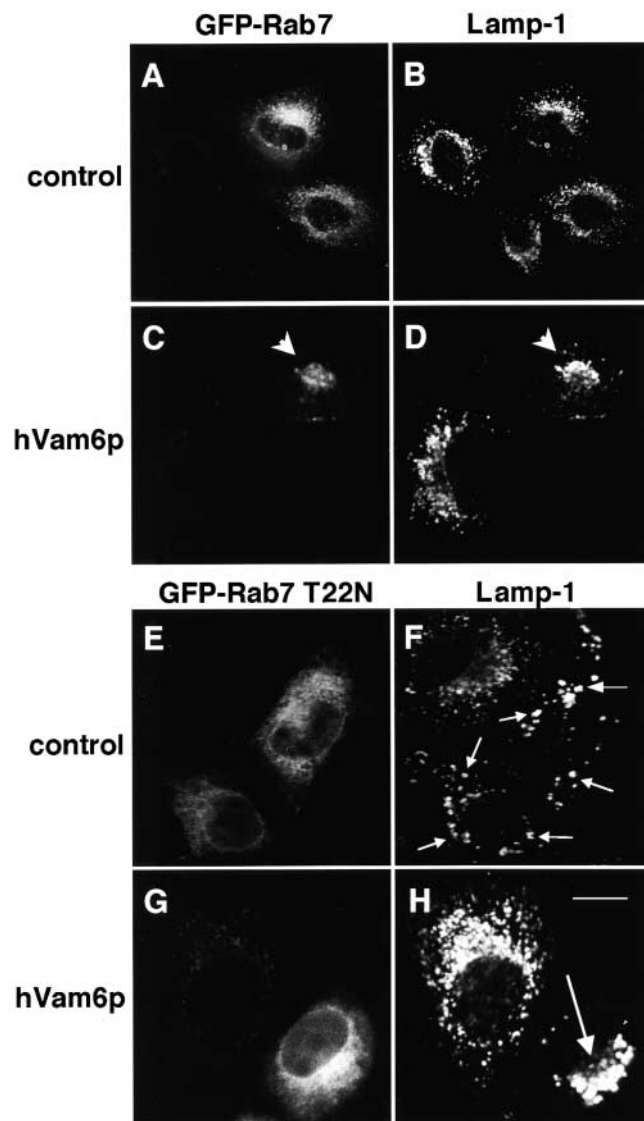
Figure 7. **hVam6p affects lysosomal morphology independently of Rab7 nucleotide cycling.** HeLa cells were transfected with either GFP–Rab7 (A and B, control) or dominant-negative GFP–Rab7 T22N (E and F, control), or were cotransfected with Myc–hVam6p together with either GFP–Rab7 (C and D) or GFP–Rab7 T22N (G and H). After 24 h, the cells were fixed-permeabilized and incubated with mouse monoclonal antibodies to lamp-1. Bound antibodies were revealed by Cy3-conjugated donkey anti–mouse IgG (B, D, F, and H), and expression of GFP–Rab7 proteins visualized by their intrinsic fluorescence (A, C, E, and G). Arrowheads depict the coalescence of both GFP–Rab7 (C) and lamp-1 (D) to a large juxtanuclear conglomerate. Small arrows (F) mark the localization of dispersed lysosomes in cells transfected with Rab7 T22N. Large arrow (H) denotes a giant juxtanuclear lysosome conglomerate in a cell overexpressing GFP–Rab7 T22N and Myc–hVam6p. Bar, 10 μm.

ysis. Sequential immunoprecipitation with antibodies to Myc and to HA demonstrated that the two epitope-tagged hVam6p proteins interacted in vivo (Fig. 9 B). The amount of total HA-tagged hVam6p coprecipitated with antibody to Myc was 10–20% in several experiments. Although this percentage may seem low, several combinations of epitope-tagged proteins can be formed, namely Myc–Myc, HA–HA, and Myc–HA. In addition, the immunoprecipitation–recap-

ture procedure is not quantitative because of the presence of some SDS in the recapture step. Accordingly, the level of Myc–HA recaptured hVam6p probably represents a significant fraction of the total hVam6p. The coprecipitation was specific, as Myc–hVam6p did not coprecipitate with HA-tagged JNK1 (Fig. 9 B). These results support the observations from the sucrose gradient analyses, indicating that hVam6p is a homooligomer.

Delineation of functional domains in hVam6p

To determine the region of hVam6p necessary for homooligomerization, a series of truncations and deletions were prepared (Fig. 9 A). HeLa cells were cotransfected with the Myc- and HA-tagged hVam6p constructs, labeled with [35S]methionine, and analyzed by immunoprecipitation–recapture (Fig. 9 B). Full-length hVam6p was found to interact with truncated hVam6p constructs lacking either the CNH domain (ΔCNH) or a COOH-terminal segment (ΔCT). However, truncation of the CLH domain in addition to the COOH-terminal segment (ΔCLH+CT) resulted in a loss of interaction with the full-length protein. These data point to a role for the CLH domain in self-assembly of hVam6p. To assess the role of the hVam6p domains in promoting lysosome clustering and fusion, we transfected Hela cells with Myc-tagged versions of full-length, ΔCT, ΔCNH, and ΔCLH+CT constructs (Fig. 9, C–N). Indirect immunofluorescence microscopy for lamp-1 demonstrated that, in addition to the full-length hVam6p (Fig. 9, C–E), the ΔCT protein (Fig. 9, F–H) also induced coalescence of lysosomes (green channel, arrows in D and G). However, loss of either the CNH domain (Fig. 9, I–K), or the COOH-terminal segment plus CLH domain of the protein (Fig. 9, L–N) completely abrogated the induction of lysosome clustering and fusion (Fig. 9, I–N). Double label immunoelectron microscopy analysis showed that both ΔCNH and ΔCLH+CT proteins lost their ability to localize to lysosomes (unpublished data), suggesting that both association with lysosomes and homo-oligomerization are requisites for inducing lysosome clustering and fusion.

Discussion

Here, we report the identification and characterization of hVam6p, a human homologue of the *S. cerevisiae* vacuolar protein sorting gene product, Vam6p. We show that overexpression of hVam6p in human cells causes coalescence of lysosomes into conglomerates of vesicles and swollen vacuoles in the vicinity of the nucleus. Many of the vesicles in the conglomerates have the appearance of multivesicular bodies and some contain the CI-MPR, suggesting that they are late endosomes. Thus, hVam6p appears to promote both homotypic and heterotypic clustering and fusion of lysosomes. Heterotypic fusion seems to be restricted to late endosomes, though, as early endosomes and other membrane-bound organelles are not affected.

Monitoring the effects of hVam6p in vivo by time-lapse imaging of fluorescently labeled lysosomes suggests a possible sequence of events. Peripheral lamp-containing vesicles (i.e., lysosomes and/or late endosomes) appear to migrate towards the juxtanuclear cytoplasm along linear tracks. These tracks
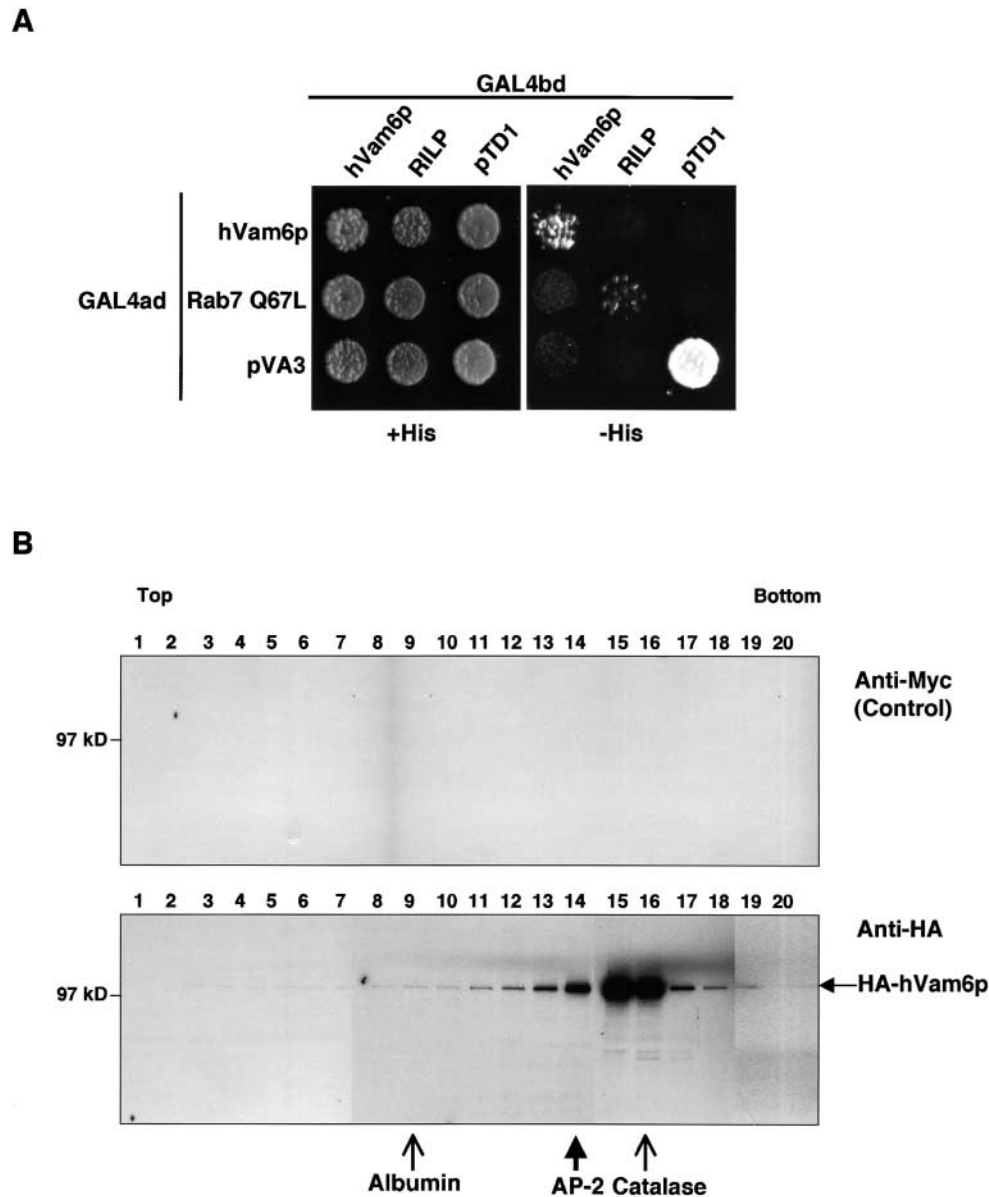
Figure 8. **Homooligomerization of hVam6p.** (A) The *S. cerevisiae* yeast strain AH109 was cotransformed with the following GAL4ad fusion constructs: GAL4ad–hVam6p, GAL4ad–Rab7 Q67L, and GAL4ad–pVA3 (murine p53 control), together with the GAL4bd fusion constructs GAL4bd–hVam6p, GAL4bd–RILP, and GAL4bd–pTD1 (SV40 large T-antigen control). Cotransformants were assayed for growth on nonselective (+His) and selective (−His) media. (B) Sedimentation velocity analysis of hVam6p from [^{35}S]methionine–labeled HeLa cells. The cell extract was run on a 4–20% sucrose gradient, and fractions were analyzed by sequential immunoprecipitations. The fractions were first cleared with an irrelevant antibody and then subjected to immunoprecipitation with a second irrelevant antibody (mouse monoclonal anti-Myc). The fractions were then immunoprecipitated with a mouse monoclonal antibody to the HA epitope. Fractions from the anti-Myc (control, top) and anti-HA (bottom) immunoprecipitations were then resolved by 4–20% gradient SDS-PAGE. Thin arrows denote markers visualized by Coomassie blue staining of separated fractions subjected to the same gradient conditions (albumin and catalase). The thick arrow denotes the position of AP-2, as visualized by immunoblotting of 10% of the labeled fractions with anti–AP-2 antibody (100/2) upon completion of the immunoprecipitations.

likely correspond to microtubules as treatment with nocodazole impairs translocation of the vesicles. Once the vesicles arrive at the juxtanuclear area, they cluster and eventually fuse with one another as well as with preexisting juxtanuclear lysosomes. Over time, the clusters and/or vesicles give rise to giant lysosomal structures reminiscent of those found in cells from patients with Chediak-Higashi syndrome (White, 1966). Few small vesicles are seen to escape from these structures, suggesting that the vesicles are irreversibly captured into the clusters. Electron microscopy analyses show that

many of the clusters are composed of a variable number of regularly shaped vesicles. Some of the clusters seem to be docked onto large vacuoles, which may precede their fusion with or engulfment into the large vacuoles.

The phenotypic effects of hVam6p overexpression are strongly suggestive of a role for hVam6p in tethering/docking events leading to fusion of lysosomes. Immunoelectron microscopy analyses show that the overexpressed hVam6p forms an electron-dense halo around vesicles containing lamp-1 and CI-MPR in the clusters. This halo resembles an
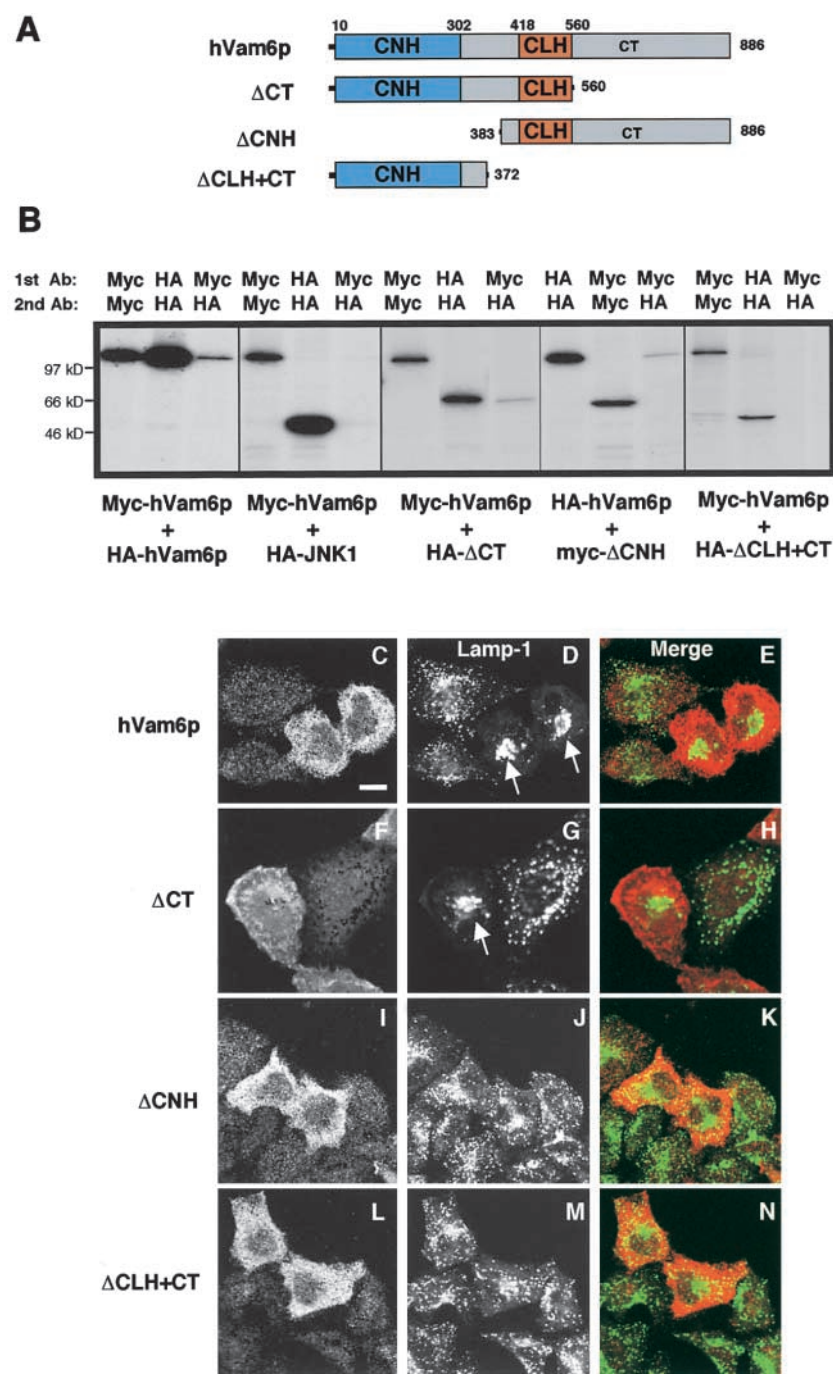
Figure 9. **Delineation of functional domains in hVam6p.** (A) Schematic representation of full-length hVam6p and various deletion constructs used in these experiments. (B) HeLa cells were cotranfected with plasmids encoding Myc– and HA–hVam6p, or hVam6p deletion mutants, or a control epitope-tagged protein (HA–JNK1), as indicated. After 18 h, cells were labeled for 8 h with [^{35}S]methionine, detergent extracted, and subjected to immunoprecipitation–recapture with the antibodies indicated. (C-N) HeLa cells were transfected with plasmids encoding Myc– or HA–Vam6p full-length or deletion constructs. After 24 h, fixed-permeabilized cells were coincubated with rabbit polyclonal antibodies to either the Myc or HA epitopes together with mouse monoclonal antibody to lamp-1. Bound antibodies were revealed by Alexa-488–conjugated donkey anti–mouse antibody (green channel) and Cy3-conjugated donkey anti–rabbit IgG (red channel). The third panel in each row was generated by merging of the images in the red and green channels. Arrows mark the coalescence of lysosomes into juxtanuclear regions. Bar, 10 μm.

exaggerated form of a filamentous coat that has been previously seen to connect the membranes of adjoining multivesicular bodies and lysosomal membranes (Futter et al., 1996). Deposition of hVam6p onto the membranes of lysosomes and late endosomes likely enhances their adhesiveness, leading to the formation of clusters. This, in turn, increases the probability of fusion resulting in the generation of large vacuoles. Thus, overexpression of hVam6p might simply augment the process by which lysosomes and late endosomes normally exchange materials through kiss-and-run (Storrie and Desjardins, 1996) or fusion–fission (Mullock et al., 1998) type of interactions.

The mechanism by which hVam6p induces lysosome clustering and fusion is still unclear. One possibility is that hVam6p may be intrinsically capable of bridging the membranes of two vesicles. Once the two vesicles are closely apposed, fusion would ensue by virtue of the SNARE-based fusion machinery. Another possibility is that overexpression of hVam6p sequesters some other factor that normally functions to prevent unregulated fusion, or to effect fission. Biochemical studies of *S. cerevisiae* Vam6p appear to support the first hypothesis, as this protein has been shown to be a component of the 38S HOPS–C-Vps complex, which mediates vacuole tethering/docking (Price et al., 2000a,b; Seals et al., 2000; Wurmser et al., 2000) and trans-SNARE pairing (Price et al., 2000b; Sato et al., 2000). HOPS–C-Vps is thought to participate in these processes as an effector of the Ypt–Rab GTPase, Ypt7 (Price et al., 2000a,b), and/or a gua-

nine nucleotide exchange factor for Ypt7 (Wurmser et al., 2000).

Several lines of evidence suggest that hVam6p may act downstream or independently of Rab7: (a) overexpression of hVam6p induces a more dramatic effect on lysosomes than overexpression of the constitutively activated Rab7 protein (unpublished data), (b) hVam6p induces lysosome clustering and fusion even in the presence of overexpressed dominant-negative Rab7 T22N, and (c) hVam6p does not interact with the constitutively activated form of Rab7. Although by analogy with yeast Vam6p, hVam6p would be expected to be a component of a putative human HOPS–C-Vps complex, data from sucrose gradients, coimmunoprecipitations, and two-hybrid analyses suggest that cytosolic hVam6p is a homooligomer. In addition, we could not detect association of hVam6p with endogenous hVam2p/Vps41p in the cytosol, and overexpression of the human Vam2p/Vps41p fails to induce effects similar to hVam6p (unpublished data). Since yeast Vam2p/Vps41p also exists as a homooligomer in the cytosol (Darsow et al., 2001), it is possible that Vam6p and Vam2p may become part of the HOPS–C-Vps complex only upon association with the vacuolar/lysosomal membrane. Based on our observations, we speculate that hVam6p may subserve the tethering/docking function of the HOPS–C-Vps complex.

Our studies have identified two functionally important domains within hVam6p: the CNH and CLH domains. The CNH domain is required for association with lysosomes and overexpression-induced lysosome clustering and fusion (Fig. 9). This suggests that the CNH domain could interact with a docking protein or with lipids on the lysosomal membrane. Other CNH domains have been shown to mediate interactions with the GTP-bound forms of the Rac and Rho GTPases (Madaule et al., 1995); although, our two-hybrid and coimmunoprecipitation analyses did not demonstrate such binding for hVam6p (unpublished data).

The CLH domain is also required for association of hVam6p with lysosomes and overexpression-induced lysosome clustering and fusion (Fig. 9). These requirements are probably related to the ability of the CLH domain to mediate homooligomerization of hVam6p (Fig. 9). CLH domains in the clathrin heavy chain (Ybe et al., 1999) and S. cerevisiae Vam2p (Darsow et al., 2001) have also been implicated in homooligomerization, suggesting that this may be the primary function of this domain. Thus, the effects of hVam6p on lysosomes appear to require homooligomerization of the protein.

In conclusion, our studies implicate hVam6p as a mammalian specific tethering/docking factor that has intrinsic ability to promote fusion of lysosomes and late endosomes in vivo. Further studies of this protein and other mammalian homologues of yeast components of the HOPS–C-Vps complex are likely to provide a greater understanding of the mechanisms involved in lysosome fusion and biogenesis.

Materials and methods

Cloning of hVam6p
A search of DNA databases identified a human homologue of S. cerevisiae Vam6p/Vps39p (KIAA0770, Nagase et al., 1998; for sequence data see GenBank/EMBL/DDBJ under accession no. AB018313.1). The complete open reading frame of this cDNA, referred to here as hVam6p (GenBank/ EMBL/DDBJ accession number AF280814), was obtained by 5′ RACE and PCR from both Marathon-Ready™ human brain and human heart cDNA libraries (CLONTECH Laboratories, Inc.), using primers designed on the basis of the partial KIAA0770 cDNA sequence. The PCR products were cloned into the pCR2.1 vector (Invitrogen) and sequenced.

Recombinant DNA constructs
Epitope tagging at the NH$_2$ terminus of hVam6p was performed by PCR amplification of the full-length hVam6p using 5′ primers containing the nucleotide sequences for the HA or Myc epitopes. These products were cloned into the EcoRV-KpnI sites of the pXS vector to yield HA–hVam6p and Myc–hVam6p constructs, respectively. A Myc-tagged construct lacking residues 1–382 (Myc–ΔCNH) was obtained by PCR amplification using a 5′ primer containing the Myc epitope nucleotide sequence and beginning with residue 383. Myc- and HA-tagged constructs encoding residues 1–560 (Myc–ΔCT) and 1–372 (HA–ΔCT+CLH) were obtained by PCR amplification using the same 5′ primer as done for Myc–hVam6p, but with a 3′ primer encoding a stop site after residues 560 and 372, respectively. For yeast two-hybrid assays, the GAL4ad–hVam6p and the GAL4bd–hVam6p constructs were prepared by ligating NdeI-BamHI PCR fragments into the multiple cloning sites of the pGADT7 (LEU2) and pGBKT7 (TRP1) vectors (CLONTECH Laboratories, Inc.). The GAL4ad–Rab7 Q67L and GAL4bd–RILP were provided by Dr. V. Deretic (University of Michigan Medical School, Ann Arbor, Michigan). GFP–lgp120 (rat lamp-1) was a gift of R. Lodge and G. Patterson (National Institutes of Health, Bethesda, MD).

Antibodies
The following monoclonal antibodies were used: HA.11 antibody to the HA epitope and 9E10 antibody to the Myc epitope (Covance), H4A3, H4B4, and anti-CD63 antibodies to lamp-1, lamp-2 and CD63, respectively (Developmental Studies Hybridoma Bank), antibody to the CI-MPR (Affinity Bioreagents), 7G7.B6 antibodies directed against the Tac epitope (American Type Culture Collection), B3/25 antibody to the human transferrin receptor (Roche Molecular Biochemicals), antitubulin antibodies, and 100/2 antibody to AP-2 (Sigma-Aldrich). Rabbit polyclonal antibodies to cathepsin D (Upstate Biotechnology) or HA and Myc epitopes (Covance) were also used.

Live imaging by time-lapse fluorescence microscopy
HeLa or COS-7 cells grown on a Lab-Tek chambered coverglass system (Nunc) were transfected with plasmids encoding either GFP–lgp120 alone or both GFP–lgp120 and HA–hVam6p, as described above. 10 h after transfection, 25 mM Hepes, pH 7.4, was added to the media, and live images of the GFP-expressing cells were obtained on a ZEISS LSM 410 confocal microscope. Temperature was maintained at 37°C with a Nev-Tek airstream stage incubator. GFP molecules were excited with the 488-nm line of a krypton–argon laser and imaged with a 527 filter. Image acquisition, processing, and automatic and manual data collection were performed using NIH Image v1.62 (Wayne Rasband Analytics). Live images are shown inverted to facilitate analysis.

Electron microscopy
For HRP-uptake studies, HeLa cells were transiently transfected on coverslips with HA–hVam6p and incubated 24 h later with 6 mg/ml HRP (Fraction VI; Sigma-Aldrich) diluted in culture medium for 4 h. Cells were fixed with 2% glutaraldehyde in 100 mM Hepes buffer (pH 7.4). HRP enzymatic activity was developed with 1% diaminobenzidine as previously described (van der Sluijs et al., 1992). Cells on coverslips were treated with reduced osmium tetroxide, dehydrated, and embedded in epoxy resin. Sections were viewed with a Philips CM-10 transmission electron microscope. For immunoelectron microscopy studies, HeLa cells were transiently transfected, fixed with 4% formaldehyde, 0.2% glutaraldehyde in 100 mM Hepes buffer (pH 7.4), and prepared for ultra-thin frozen sectioning as described (Slot et al., 1991).

Other procedures
Human HeLa cells were grown on glass coverslips, transfected using FUGENE-6 (Roche Molecular Biochemicals), and either fixed and processed for immunofluorescence (Dell'Angelica et al., 1997), or used directly for analysis of rhodamine–dextran or LysoTracker™ (Molecular Probes) uptake, followed by fixation and processing, as described above. Microtubule disruption was induced by treatment with 0.5 μM nocodazole (Sigma-Aldrich) for 16 h, immediately after transfection. All images were obtained using a ZEISS LSM 410 confocal microscope. Northern blot analysis (Dell'Angelica et al., 1997), metabolic labeling, cell surface biotinylation (Caplan et al., 2000), sedimentation analysis (Dell'Angelica et al., 1997), and yeast

two-hybrid assays (Aguilar et al., 1997) using the strain AH109 (CLON-TECH Laboratories, Inc.) were performed as previously described.

Online supplemental material

Online supplemental materials are available at http://www.jcb.org/cgi/content/full/200102142/DC1. Video 1 corresponds to Fig. 6 A and contains a Quicktime movie sequence depicting the centripetal movement and fusion of GFP–lamp-1–containing vesicles in a COS-7 cell also expressing hVam6p. Images were captured every 30 s over the course of 31 min. Video 2 corresponds to Fig. 6 B and contains a Quicktime movie sequence demonstrating fusion of a peripheral GFP–lamp-1–containing organelle with a large juxtanuclear lysosomal structure in a HeLa cell also expressing hVam6p. Images were captured every 30 s over the course of 200 min. Video 3 corresponds to Fig. 6 C and contains a Quicktime movie sequence illustrating the centripetal movement and alignment of GFP–lamp-1 structures from the periphery along the juxtanuclear axis of a COS-7 cell expressing hVam6p. Images were captured every minute over the course of 388 min.

References

Aguilar, R.C., H. Ohno, K.W. Roche, and J.S. Bonifacino. 1997. Functional mapping of the clathrin-associated adaptor medium chains μ1 and μ2. *J. Biol. Chem.* 272:27160–27166.

Bakker, A.C., P. Webster, W.A. Jacob, and N.W. Andrews. 1997. Homotypic fusion between aggregated lysosomes triggered by elevated [Ca²⁺]i in fibroblasts. *J. Cell Sci.* 110:2227–2238.

Bucci, C., P. Thomsen, P. Nicoziani, J. McCarthy, and B. van Deurs. 2000. Rab7: a key to lysosome biogenesis. *Mol. Biol. Cell.* 11:467–480.

Cantalupo, G., P. Alifano, V. Roberti, C.B. Bruni, and C. Bucci. 2001. Rab-interacting lysosomal protein (RILP): the Rab7 effector required for transport to lysosomes. *EMBO J.* 20:683–693.

Caplan, S., E.C. Dell'Angelica, W.A. Gahl, and J.S. Bonifacino. 2000. Trafficking of major histocompatibility complex class II molecules in human B-lymphoblasts deficient in the AP-3 adaptor complex. *Immunol. Lett.* 72:113–117.

Charng, M.J., D. Zhang, P. Kinnunen, and M.D. Schneider. 1998. A novel protein distinguishes between quiescent and activated forms of the type I transforming growth factor β receptor. *J. Biol. Chem.* 273:9365–9368.

Dan, I., N.M. Watanabe, T. Kobayashi, K. Yamashita-Suzuki, Y. Fukagaya, E. Kajikawa, W.K. Kimura, T.M. Nakashima, K. Matsumoto, J. Ninomiya-Tsuji, and A. Kusumi. 2000. Molecular cloning of MINK, a novel member of mammalian GCK family kinases, which is up-regulated during postnatal mouse cerebral development. *FEBS Lett.* 469:19–23.

Darsow, T., D. Katzmann, C.R. Cowles, S.D. Emr. 2001. Vps41p function in the alkaline phosphatase pathway requires homo-oligomerization and interaction with AP-3 through two distinct domains. *Mol. Biol. Cell.* 12:37–51.

Dell'Angelica, E.C., H. Ohno, C.E. Ooi, E. Rabinovich, K.W. Roche, and J.S. Bonifacino. 1997. AP-3: an adaptor-like protein complex with ubiquitous expression. *EMBO J.* 15:917–928.

Eitzen, G., E. Will, D. Gallwitz, A. Haas, and W. Wickner. 2000. Sequential action of two GTPases to promote vacuole docking and fusion. *EMBO J.* 19:6713–6720.

Fu, C.A., M. Shen, B.C. Huang, J. Lasaga, D.G. Payan, and Y. Luo. 1999. TNIK, a novel member of the germinal center kinase family that activates the c-Jun N-terminal kinase pathway and regulates the cytoskeleton. *J. Biol. Chem.* 274:30729–30737.

Funato, K., W. Beron, C.Z. Yang, A. Mukhopadhyay, and P.D. Stahl. 1997. Reconstitution of phagosome-lysosome fusion in streptolysin O-permeabilized cells. *J. Biol. Chem.* 272:16147–16151.

Futter, C.E., A. Pearse, L.J. Hewlett, and C.R. Hopkins. 1996. Multivesicular endosomes containing internalized EGF–EGF receptor complexes mature and then fuse directly with lysosomes. *J. Cell Biol.* 132:1011–1023.

Kornfeld, S., and I. Mellman. 1989. The biogenesis of lysosomes. *Annu. Rev. Cell Biol.* 5:483–525.

Letourneur, F., and R.D. Klausner. 1992. A novel di-leucine motif and a tyrosine-based motif independently mediate lysosomal targeting and endocytosis of CD3 chains. *Cell.* 69:1143–1157.

Luzio, J.P., B.A. Rous, N.A. Bright, P.R. Pryor, B.M. Mullock, and R.C. Piper. 2000. Lysosome-endosome fusion and lysosome biogenesis. *J. Cell Sci.* 113:1515–1524.

Madaule, P., T. Furuyashiki, T. Reid, T. Ishizaki, G. Watanabe, N. Morii, and S. Narumiya. 1995. A novel partner for the GTP-bound forms of rho and rac. *FEBS Lett.* 377:243–248.

Mullock, B.M., N.A. Bright, C.W. Fearon, S.R. Gray, and J.P. Luzio. 1998. Fusion of lysosomes with late endosomes produces a hybrid organelle of intermediate density and is NSF dependent. *J. Cell Biol.* 140:591–601.

Mullock, B.M., C.W. Smith, G. Ihrke, N.A. Bright, M. Lindsay, E.J. Parkinson, D.A. Brooks, R.G. Parton, D.E. James, J.P. Luzio, and R.C. Piper. 2000. Syntaxin 7 is localized to late endosome compartments, associates with vamp 8, and is required for late endosome-lysosome fusion. *Mol. Biol. Cell.* 11:3137–3153.

Nagase, T., K. Ishikawa, M. Suyama, R. Kikuno, N. Miyajima, A. Tanaka, H. Kotani, N. Nomura, and O. Ohara. 1998. Prediction of the coding sequences of unidentified human genes. XI. The complete sequences of 100 new cDNA clones from brain which code for large proteins in vitro. *DNA Res.* 5:277–286.

Nakamura, N., A. Hirata, Y. Ohsumi, and Y. Wada. 1997. Vam2/Vps41p and Vam6/Vps39p are components of a protein complex on the vacuolar membranes and involved in the vacuolar assembly in the yeast *Saccharomyces cerevisiae. J. Biol. Chem.* 272:11344–11349.

Novick, P., and M. Zerial. 1997. The diversity of Rab proteins in vesicle transport. *Curr. Opin. Cell Biol.* 9:496–504.

Price, A., D. Seals, W. Wickner, and C. Ungermann. 2000a. The docking stage of yeast vacuole fusion requires the transfer of proteins from a cis-SNARE complex to a Rab/Ypt protein. *J. Cell Biol.* 148:1231–1238.

Price, A., W. Wickner, and C. Ungermann. 2000b. Proteins needed for vesicle budding from the Golgi complex are also required for the docking step of homotypic vacuole fusion. *J. Cell Biol.* 148:1223–1229.

Pryor, P.R., B.M. Mullock, N.A. Bright, S.R. Gray, and J.P. Luzio. 2000. The role of intraorganellar Ca²⁺ in late endosome–lysosome heterotypic fusion and in the reformation of lysosomes from hybrid organelles. *J. Cell Biol.* 149:1053–1062.

Sato, T.K., P. Rehling, M.R. Peterson, and S.D. Emr. 2000. Class C Vps protein complex regulates vacuolar SNARE pairing and is required for vesicle docking/fusion. *Mol. Cell.* 6:661–671.

Seals, D.F., G. Eitzen, N. Margolis, W.T. Wickner, and A. Price. 2000. A Ypt/Rab effector complex containing the Sec1 homolog Vps33p is required for homotypic vacuole fusion. *Proc. Natl. Acad. Sci. USA.* 97:9402–9407.

Slot, J.W., H.J. Geuze, S. Gigengack, G.E. Lienhard, and D.E. James. 1991. Immunolocalization of the insulin regulatable glucose transporter in brown adipose tissue of the rat. *J. Cell Biol.* 113:123–135.

Sollner, T.H., and J.E. Rothman. 1996. Molecular machinery mediating vesicle budding, docking and fusion. *Experientia.* 52:1021–5.

Storrie, B., and M. Desjardins. 1996. The biogenesis of lysosomes: is it a kiss and run, continuous fusion and fission process? *Bioessays.* 18:895–903.

Ungermann, C., G.F. von Mollard, O.N. Jensen, N. Margolis, T.H. Stevens, and W. Wickner. 1999. Three v-SNAREs and two t-SNAREs, present in a pentameric cis-SNARE complex on isolated vacuoles, are essential for homotypic fusion. *J. Cell Biol.* 145:1435–1442.

Ungermann, C., A. Price, and W. Wickner. 2000. A new role for a SNARE protein as a regulator of the Ypt7/Rab-dependent stage of docking. *Proc. Natl. Acad. Sci. USA.* 97:8889–8891.

van der Sluijs, P., M. Hull, P. Webster, P. Male, B. Goud, and I. Mellman. 1992. The small GTP-binding protein rab4 controls an early sorting event on the endocytic pathway. *Cell.* 70:729–740.

Ward, D.M., J.D. Leslie, and J. Kaplan. 1997. Homotypic lysosome fusion in macrophages: analysis using an in vitro assay. *J. Cell Biol.* 139:665–673.

Ward, D.M., J. Pevsner, M.A. Scullion, M. Vaughn, and J. Kaplan. 2000. Syntaxin 7 and VAMP-7 are soluble *N*-ethylmaleimide-sensitive factor attachment protein receptors required for late endosome-lysosome and homotypic lysosome fusion in alveolar macrophages. *Mol. Biol. Cell.* 11:2327–2333.

Waters, M.G., and S.R. Pfeffer. 1999. Membrane tethering in intracellular transport. *Curr. Opin. Cell Biol.* 11:453–459.

White, J.G. 1966. The Chediak-Higashi syndrome: a possible lysosomal disease. *Blood.* 28:143–156.

Wickner, W., and A. Haas. 2000. Yeast homotypic vacuole fusion: a window on organelle trafficking mechanisms. *Ann. Rev. Biochem.* 69:247–275.

Wurmser, A.E., T.K. Sato, and S.D. Emr. 2000. New component of the vacuolar class C-Vps complex couples nucleotide exchange on the ypt7 GTPase to SNARE-dependent docking and fusion. *J. Cell Biol.* 151:551–562.

Ybe, J.A., F.M. Brodsky, K. Hofmann, K. Lin, S.H. Liu, L. Chen, T.N. Earnest, R.J. Fletterick, and P.K. Hwang. 1999. Clathrin self-assembly is mediated by a tandemly repeated superhelix. *Nature.* 399:371–375.

Zimmerli, S., M. Majeed, M. Gustavsson, O. Stendahl, D.A. Sanan, and J.D. Ernst. 1996. Phagosome–lysosome fusion is a calcium-independent event in macrophages. *J. Cell Biol.* 132:49–61.